Does local chain conformation affect the chiral recognition ability of an amylose derivative? Comparison between linear and cyclic amylose tris(3,5-dimethylphenylcarbamate)

Akiyuki Ryoki,[a,1] Yuto Kimura,[a] Shinichi Kitamura,[b] Katsuhiro Maeda,[c] and Ken Terao[a,*]

[a] *Department of Macromolecular Science, Graduate School of Science, Osaka University, 1-1 Machikaneyama-cho, Toyonaka, Osaka 560-0043, Japan*
[b] *Graduate School of Life and Environmental Sciences, Osaka Prefecture University, Gakuen-cho, Nakaku, Sakai, Osaka 599-8531, Japan*
[c] *Nano Life Science Institute (WPI NanoLSI), Kanazawa University, Kakuma-machi, Kanazawa 920-1192, Japan*

* Corresponding Author.
E-mail address: kterao@chem.sci.osaka-u.ac.jp
[1] Present address: Department of Polymer Chemistry, Graduate School of Engineering, Kyoto University, Kyoto, Japan.

Highlights
Coated and immobilized columns were prepared from linear ADMPC and cyclic cADMPC.
Coated cADMPC columns have different chiral separation ability from that of ADMPC.
Separation ability of cADMPC columns resembles that of immobilized ADMPC columns.
Local conformation plays an important role for the chiral separation.

ABSTRACT
Coated-type chiral stationary phases (CSPs) for high-performance liquid chromatography (HPLC) were prepared from three cyclic amylose tris(3,5-dimethylphenylcarbamate) (cADMPC) samples, of which weight-average molar mass (M_w) ranges from 19 to 91 kg mol^{-1}, and from three linear ADMPC samples ranging in M_w from 25 to 90 kg mol^{-1}. CSPs made of cADMPC showed appreciably different chiral separation ability comparing with those for ADMPC with a mixed eluent of *n*-hexane and 2-propanol. Local conformation plays an important role for the chiral separation taking into account that the local helical structure of cADMPC in dilute solution is extended comparing with ADMPC. Immobilized-type CSPs were also prepared from enzymatically synthesized linear and cyclic amylose samples with 3-(triethoxysilyl)propylcarbamate linkers (ADMPCi and cADMPCi) of which M_w's are in the range from 18 to 130 kg mol^{-1}. When we choose quite high linker contents, CSPs of cADMPCi were fairly close to those of ADMPCi. This suggests that local conformations of ADMPCi and cADMPCi are similar in the stationary phase since they are crosslinked to the other polymer chains with multiple points on the polymer chain.

Key Words: Chiral HPLC, Chiral stationary phase, Linear amylose, Cyclic amylose, Immobilization

1. Introduction

An amylose derivative, amylose tris(3,5-dimethylphenylcarbamate) (ADMPC) of which chemical structure is shown in Fig. 1(A) is widely used as a chiral selector in high-performance liquid chromatography (HPLC) [1]. For example, their separation behavior was widely investigated on the basis of the quantitative structure-enantioselective retention relationships [2-5]. The chiral separation mechanism was also investigated by ^{1}H NMR, infrared spectroscopy, X-ray diffraction, and molecular modelling [6-8]. Supercritical fluid chromatography of ADMPC columns was also investigated to clarify the separation mechanism [9-11]. According to these reports, intermolecular interactions between side groups of polysaccharide derivatives and enantiomer molecules play an important role for the chiral recognition. However, it is still unclear whether the conformational change of polysaccharide derivative may cause significant difference to the chiral separation behavior.

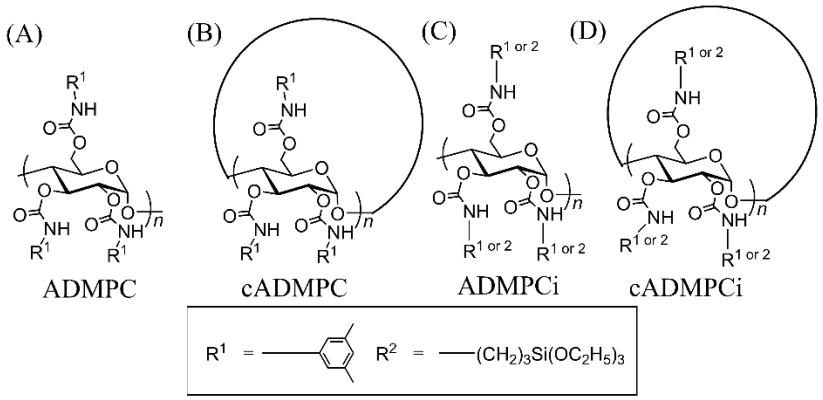

Fig. 1. Chemical structures of ADMPC (A), cADMPC (B), ADMPCi (C) and cADMPCi (D).

We recently found that linear and cyclic ADMPC has appreciably different local conformation in solution [12], in that the local helical structure of cyclic ADMPC [cADMPC, Fig. 1(B)] is more extended than linear ADMPC as schematically illustrated in Fig. 2. Furthermore, according to Aburatani et al. [13], the chiral recognition ability of oligo ADMPC with 4 – 7 repeat units were not so different from that of ADMPC, but cyclodextrin-based cyclic ADMPC's have quite different recognition ability from that of ADMPC. Investigation of chiral stationary phase consisting of cADMPC may therefore clarify the relationship between the local conformation and chiral separation ability.

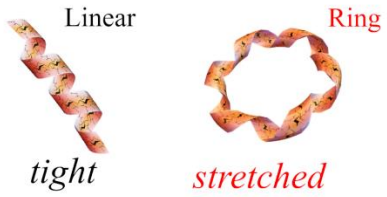

Fig. 2. Schematic illustration of the difference in the helical structure between ADMPC and cADMPC.

We thus prepared physically-coated chiral-stationary phases (CSPs) of cADMPC samples of which weight-average molar mass M_w ranges between 19 and 91 kg mol^{-1}. CSPs were also

prepared for linear ADMPC samples to compare the chiral separation ability. The performance of the CSPs was characterized with 8 racemates. We also prepared chemically-immobilized CSPs with cADMPC and ADMPC to reveal the local conformational effects on the chiral separation ability since chain conformation of ADMPC chains between two linkers may be restricted. We thus chose higher linker contents that those for previously investigated immobilized columns [14] to accentuate the chain constraint effects on the chiral separation ability.

2. Materials and methods

2.1. Chemical reagents

A wide-pore silica gel (Daiso gel SP-1000-7, Osaka Soda, Osaka, Japan) with a mean particle diameter of 7 μm and a mean pore size of 100 nm was purchased from Osaka Soda. Toluene (Fujifilm Wako Pure Chemical, Osaka, Japan), pyridine (Fujifilm), and methyl acetate (MEA, Kishida Chemical, Osaka, Japan) were distilled over calcium hydride (Nacalai Tesque, Kyoto, Japan) before use. 3-Aminopropyltriethoxysilane (TCI chemical, Tokyo, Japan), 3,5-dimethylphenyl isocyanate (TCI), 3-(triethoxysilyl)propyl isocyanate (TCI), chlorotrimethylsilane (TCI), *N*,*N*-dimethylformamide-d_7 (Sigma-Aldrich Japan, Tokyo, Japan), *N,N*-dimethylacetamide (dehydrated grade, Fujifilm), lithium chloride (Fujifilm), acetone (Fujifilm), methanol (Fujifilm), *n*-hexane (Fujifilm), *n*-tetradecane (Fujifilm), and 2-propanol (HPLC grade, Fujifilm) were used without further purification. Racemate samples, *trans*-stilbene oxide (Sigma), Tröger's base (Fujifilm), 2,2,2-trifluoro-1-(9-anthryl)ethanol (TCI), flavanone (TCI), tris(2,4-pentanedionato)cobalt(III) (TCI), benzoin (Fujifilm), 1,1'-bi-2-naphthol (TCI), and 1-(2-Naphthyl)ethanol (TCI), and reference materials, benzene (spectrochemical-analysis grade, Fujifilm) and 1,3,5-tri-*tert*-butylbenzene (TCI) for HPLC measurements were purchased and used without further purification. Linear enzymatically synthesized amylose (ESA) was synthesized by the previously reported method [15]. Cyclic amylose (cESA) was synthesized enzymatically from ESA [16].

2.2. Cyclic and linear amylose carbamate samples

Previously investigated three cADMPC samples [12], **cADMPC19K**, **cADMPC49K**, and **cADMPC91K**, and two ADMPC samples [17], **ADMPC25K** and **ADMPC49K** were used for this study. The values of M_w are summarized in Table 1. Their dispersity index $Đ$ defined as M_w/M_n was estimated to be from 1.04 to 1.20, with M_n being the number-average molar mass. The degree of substitution DS_{R1} of 3,5-dimethylphenylcarbamate group was determined to be 2.9 – 3.3 from the ultimate analysis [12, 17]. Another ADMPC sample, **ADMPC90K**, was newly synthesized from an ESA sample in the manner reported previously [17]. The chemical structure of **ADMPC90K** was confirmed by ^{1}H NMR in deuterated chloroform with a JEOL ECS-400 FT-NMR spectrometer (400 MHz for ^{1}H-NMR, JEOL, Tokyo, Japan) and ultimate analysis with an MT-5 CHN analyzer (Yanaco, Kyoto, Japan) . The M_w value was estimated from the intrinsic viscosity $[\eta]$ (= 36.0 mL g^{-1}) in MEA at 25 °C with the known $[\eta] - M_w$ relationship [17]. A Ubbelohde type viscometer was used to determine $[\eta]$.

A cADMPCi sample, **cADMPCi31K**, of which chemical structure is shown in Fig. 1(D) was prepared in the manner reported elsewhere [12, 18]. The procedure is as follows. A cESA sample (M_w = 9 kg mol^{-1}, 2.1 g, 13 mmol of the repeat unit) and lithium chloride (2.1 g) were dried in a vacuum at 100 °C for 6 h. *N*,*N*-Dimethylacetamide (40 mL) was added to them and stirred at 90 °C under Ar atmosphere to dissolve both lithium chloride and amylose. Pyridine (80 mL) and 3,5-dimethylphenyl isocyanate (5.0 mL, 35 mmol) were added to the reaction mixture. It

was stirred at 80 °C for 6 h. After 3-(triethoxysilyl)propyl isocyanate (1.3 mL, 5.3 mmol) was added, the mixture was further stirred at 80 °C overnight. In order to diminish residual hydroxyl groups on the glucosidic ring, we further added 3,5-dimethylphenyl isocyanate (5.0 mL) to the resultant solution and stirred at 80 °C for 6 h. The crude product was poured into an excess amount of methanol at room temperature to purify the polymer sample as a precipitant. The chemical structure of **cADMPCi31K** was confirmed by ^{1}H NMR in fully deuterated *N*,*N*-dimethylformamide at 80 °C. While possible impurities, amine and urethane, were estimated to be at most 1 – 7 wt% in each sample, we did not further purify the samples to protect the linker group. This may not substantially affect the performance of CSPs because the chiral columns will be washed with large amount of eluent before use. The degree of substitution DS_{R2} of the 3-(triethoxysilyl)propylcarbamate group (R^2) of **cADMPCi31K** was determined from the peak area ratio of the protons of SiH_2 group on R^2 to the aromatic protons on the 3,5-dimtheylcarbamate group (R^1). The M_w value was determined to be 31 kg mol^{-1} from SAXS measurements as described later.

Table 1. Weight-average molar mass Mw and degree of substitution DSR2 of amylose carbamate samples used for the chiral stationary phase

samples	M_w (kg mol^{-1})	DS_{R2}
cADMPC19K	19.4[a]	0
cADMPC49K	49.4[a]	0
cADMPC91K	91.1[a]	0
ADMPC25K	25.4[b]	0
ADMPC49K	48.8[b]	0
ADMPC90K	90[c]	0
cADMPCi31K	31[c]	0.30
ADMPCi18K	18[c]	0.14
ADMPCi20K	20[c]	0.23
ADMPCi130K	130[c]	0.24

[a] Ref. [12]. [b] Ref. [17]. [c] This work.

We have also prepared three ADMPCi samples [see Fig. 1(C) for the chemical structure], **ADMPCi18K**, **ADMPCi20K**, and **ADMPCi130K** from two enzymatically synthesized amylose samples in the similar manner as that for **cADMPCi31K**. Ultimate analysis and ^{1}H NMR measurements were performed to confirm the chemical structure. Viscosity measurements were made for the three samples in MEA at 25 °C to determine $[\eta]$ to be 7.45, 7.75, and 44.2 mL g^{-1} and the Huggins constant to be 0.82, 0.77, and 0.43 for **ADMPCi18K**, **ADMPCi20K**, and **ADMPCi130K**, respectively. Assuming that $[\eta]M_0$ for the ADMPCi samples with M_0 being average molar mass per monosaccharide unit are the same as that for ADMPC with the same

M_w/M_0, the M_w values for the three ADMPCi samples were estimated from the known relationship between $[\eta]$ and M_w for ADMPC [17] as listed in Table 1 along with DS_{R2}. This is reasonable because the wormlike chain parameters discussed later are substantially close to those for the ADMPC in the same solvent.

2.3. Small-angle X-ray scattering (SAXS) of dilute solution

In order to compare the conformation of the amylose carbamate samples with or without triethoxysilyl groups, synchrotron-radiation SAXS measurements were made for **cADMPCi31K** and **ADMPCi130K** in MEA at 25 °C at the BL40B2 beamline in SPring-8 to determine the excess scattering intensity $\Delta I(q)$ as functions of the magnitude q of the scattering vector and the polymer mass concentration c. Solvent and the four solutions of which c ranged between 2.2 and 11 mg mL^{-1} were measured with the same quartz capillary cell to extrapolate $\Delta I(q)/c$ to infinite dilution. The scattered light was detected by a Dectris PILATUS3S 2M detector (Dectris, Baden, Switzerland) for 120 s for each solution. The wavelength of the incident light and the camera length were set to be 0.1 nm and 4 m, respectively. The beam center on the detector and the actual camera length were determined from the Bragg reflection of silver behenate by means of the SAngular software [19]. Data analysis for **cADMPCi31K** and **ADMPCi130K** was substantially the same as those for cADMPC [12] and ADMPC [17] to determine the z-average mean-square radius of gyration $\langle S^2 \rangle_z$ and the particle scattering function $P(q)$. We also estimated M_w of **cADMPCi31K** from the doubly extrapolated scattering intensity $[\Delta I(0)/c]_{c\to 0}$ to both $c = 0$ and $q = 0$ by using that for **ADMPCi130K** assuming the excess electron density of the two samples are identical.

2.4. Preparation of chiral stationary phases (CSPs) and chiral columns

We prepared 10 CSPs from the samples in Table 1, that is, six coated-type CSPs and four immobilized-type CSPs. All chiral stationary phases (CSPs) were made from the same macroporous silica gel (Daiso gel SP-1000-7) to compare the chiral recognition ability among the polysaccharide derivative samples. The detailed procedure is as follows.

2.4.1. Preparation of coated-type stationary phases

Six coated-type CSPs were prepared from **ADMPC25K**, **ADMPC49K**, **ADMPC90K**, **cADMPC18K**, **cADMPC49K**, and **cADMPC91K** in the manner reported by Okamoto et al. [20]. A typical procedure is as follows. The silica gel (25 g) was dried under vacuum at 100 °C overnight and mixed with toluene (240 mL) in a two-necked flask at 80 °C under Ar atmosphere. A mixture of 3-aminopropyltriethoxysilane (51 g) and toluene (40 mL) was dropped into the silica-gel suspension. The resultant suspension was kept at 80 °C for 5 h to complete the reaction to obtain 3-amynopropyltriethoxisilinized silica gel (A-silica) [21, 22], which was washed four times with toluene (100 mL each) and four times with methanol (100 mL each). The resultant crude sample was dispersed into a mixture of water (100 mL) and methanol (100 mL) by sonication for 2 min. The suspension was kept at room temperature for 2 h to eliminate the remaining ethoxy groups [22]. The obtained A-silica sample was washed three times by methanol (100 mL each) and dried under reduced pressure. An MEA solution (11 mL) of **cADMPC49K** (0.23 g) was mixed with the A-silica sample (0.92 g) and the solvent was evaporated in an eggplant flask. The obtained CSP was dried in a vacuum overnight.

2.4.2. Preparation of immobilized-type stationary phases

Four immobilized-type CSPs were synthesized from **cADMPCi31K**, **ADMPCi18K**, **ADMPCi20K**, and **ADMPCi130K** with the cross-linking method on silica particles following the procedure reported by Ikai et al. [18]. A sample, **cADMPCi31K** (0.70 g), was dissolved in pyridine (8 mL) and mixed with the silica gel (Daiso gel SP-1000-7, 2.8 g). The solvent was evaporated from the mixture and the resultant sample was dried in a vacuum overnight to physically coat **cADMPCi31K** on silica particles. The obtained product (1.95 g) was mixed with ethanol (18 mL), water (4.5 mL), and chlorotrimethylsilane (0.3 mL). The mixture was kept under reflux condition at 110 °C for 10 min to immobilize the polymer chains. The obtained CSP was washed with an excess amount of acetone and MEA to remove impurities including free **cADMPCi31K** molecules. Thermogravimetric analyses showed that about 90 % of **ADMPCi20K**, and **ADMPCi130K** or 70 % of **cADMPCi31K** and **ADMPCi18K** were immobilized on the silica surface.

2.4.3. Preparation of chiral columns

Each stationary phase was packed in a stainless steel column (Senshu Scientific, Tokyo, Japan) with 2.1 mm of the inner diameter and 250 mm of the length by using a slurry method. 2-Propanol was chosen as an eluent to pack CSPs with **cADMPC49K**, **cADMPC91K**, **ADMPC49K**, **ADMPC90K**, **cADMPCi31K**, **ADMPCi18K**, **ADMPCi20K**, and **ADMPCi130K**. Tetradecane including 2% 2-propanol (volume fraction) was chosen as the eluent to fill the CSPs of **cADMPC19K** and **ADMPC25K** due to slight but non-negligible solubility of the polysaccharide derivatives in 2-propanol. A typical procedure is as follows. A CSP of **cADMPC49K** (0.9 g) was sonicated in 2-propanol (30 mL) to be dispersed. The obtained suspension was filtered with a stainless steel mesh (270 mesh) and incubated at room temperature for 1 h to precipitate the CSP, which was washed with 2-propanol (30 mL) again. The resultant CSP was dispersed in 2-propanol (30 mL) and filled into the column with a specially designed column packer and a DP-8020 HPLC pump (Tosoh, Tokyo, Japan). The flow rate was set to be 1.0 mL min^{-1} to achieve the back pressure of 32 MPa for about 4 h.

2.5. High-performance liquid chromatography (HPLC) of the CSPs

Chiral separation performance of the ten columns prepared from the CSPs listed in Table 1 were tested with the following racemates, *trans*-stilbene oxide (**a**), Tröger's base (**b**), 2,2,2-trifluoro-1-(9-anthryl)ethanol (**c**), flavanone (**d**), tris(2,4-pentanedionato)cobalt(III) (**e**), benzoin (**f**), 1,1'-bi-2-naphthol (**g**), and 1-(2-Naphthyl)ethanol (**h**) of which chemical structures are summarized in Fig. 3. Tröger's base **b** contains two bridgehead stereogenic nitrogen atoms, there are two enantiomers for the cobalt complex **e**, and 1,1'-bi-2-naphthol **g** has axial chirality of which two enantiomers are stable toward racemization.

Each column was installed into an HPLC system equipped with a Chromaster 5160 pump (Hitachi, Tokyo, Japan), a Rheodyne 7125 injector with a 20 μL sample loop, an online UV absorption detector (UV-8001, Tosoh) with the wavelength λ_0 = 254 nm in a vacuum, and an SF-3120 fraction collector (Advantec, Tokyo, Japan). The column temperature was controlled to be 25.0 ± 0.1 °C using a thermostated water bath. The 7 columns, made of **cADMPC49K**, **cADMPC91K**, **ADMPC49K**, **ADMPC90K**, **cADMPCi31K**, **ADMPCi20K**, and **ADMPCi130K** were tested with the mobile phase of hexane/2-propanol (9/1) at the flow rate of 0.05 and 0.1 mL min^{-1} to separate all the 8 racemates. The 8 columns, made of **cADMPC19K**, **cADMPC49K**, **cADMPC91K**, **ADMPC25K**, **ADMPC49K**, **ADMPC90K**, **ADMPCi18K**, and

ADMPCi130K were tested with *n*-hexane/2-propanol (99/1) at 0.1 and 0.2 mL min^{-1} to separate **a–e** and **h**. Noted that **cADMPC19K** and **ADMPC25K** are not applicable for the former mobile phase due to the slightly higher solubility and the solubility of the two racemates, **f** and **g**, was poor to the latter eluent.

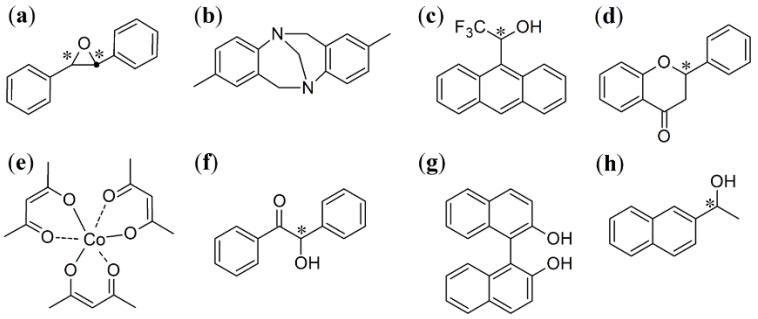

Fig. 3. Chemical structures of the racemates (**a**-**h**) investigated.

The plate number N and the dead volume V_0 of the columns were estimated from the peak shape of benzene and 1,3,5-tri-*tert*-butylbenzene, respectively. While the latter was evaluated to be $V_0 = 0.6 – 0.7$ mL and mostly independent both of the eluent and the flow rate investigated, the former was estimated to be between $N = 350$ and 2300 and appreciably decreased with increasing the flow rate when the flow rate exceeded 0.1 mL min^{-1}. When we obtained two peaks in the chromatogram, circular dichroism (CD) measurements were made on a J-720WO CD spectrometer (Jasco, Tokyo, Japan) to characterize each fraction in the ultraviolet region ($\lambda_0 = 210 – 350$ nm) except for **h** which does not show appreciable CD signal. One of the fractions having negative CD signal at the highest λ_0 was designated to be E– and the other was named E+; see Fig. S2 for the CD spectra. Retention volumes were determined as the peak-top positions for each chromatogram to estimate capacity factors $k_{E–}$ and k_{E+} for E– and E+, respectively.

3. Results and discussion

3.1. Conformation of cADMPCi and ADMPCi in MEA

Fig. 4 shows that the $\langle S^2 \rangle_z^{1/2}$ data for **ADMPCi130K** and **cADMPCi31K** in MEA at 25 °C plotted against M_w/M_0, where M_0 is the average molar mass of the repeat unit ($M_0 = 0.628$ kg mol^{-1} for **ADMPCi130K** and $M_0 = 0.634$ kg mol^{-1} for **cADMPCi31K**). The obtained data are substantially the same as those without linkers.

Fig. 5 illustrates the Holtzer plot for **ADMPCi130K** in MEA at 25 °C. Since the shape is typical for the wormlike chain with finite thickness, the data was analyzed in terms of the wormlike cylinder model [23] as in the case of ADMPC in the same solvent [17]. A curve fitting procedure was employed to determine the Kuhn segment length λ^{-1}, the contour length per residue h, and the chain diameter d as 20 ± 4 nm, 0.39 ± 0.03 nm, and 1.6 ± 0.2 nm, respectively. The theoretical solid curve in Fig. 5 well explains the experimental data. The obtained parameters are essentially the same as those for ADMPC in the same solvent, that is, $\lambda^{-1} = 22 \pm 2$ nm, $h = 0.36 \pm 0.02$ nm, and $d = 1.3 \pm 0.1$ nm, indicating the conformation of **ADMPCi130K** in MEA is substantially the same as those for ADMPC.

The $P(q)$ data for **cADMPCi31K** in MEA is shown in Fig. 6. The shape is similar to that for cADMPC [12] with substantially the same chain length. The data was analyzed in terms of the

touched-bead wormlike ring model which is characterized by λ^{-1}, h, and the bead diameter d_b. The detailed procedure including the computer program developed by Tsubouchi et al. [24] was described in Ref. [25]. If we choose λ^{-1} = 13 nm, h = 0.41 nm, and d_b = 1.7 nm, the theoretical dot-dashed curve in Fig. 6 significantly fluctuates. A reason for the disagreement is due to the molar mass distribution. Indeed, if we assume $Đ$ = 1.2, the resultant theoretical solid curve in the figure satisfactory reproduce the experimental data. We determined h = 0.38 ± 0.04 nm and d_b = 1.8 ± 0.2 nm from the curve fitting method. It should be noted that we only estimated the lowest limit of λ^{-1} to be 13 nm since the theoretical rigid limiting value (dashed curve) is substantially close to that for the wormlike ring. Nevertheless, the obtained parameters are consistent with those for **cADMPC31K** of which chain length is essentially close to that for the current **cADMPCi31K**, indicating substantially the same conformation.

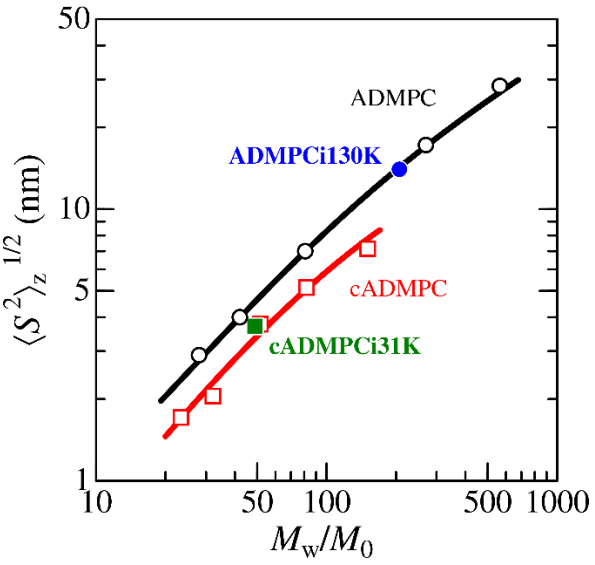

Fig. 4. M_w/M_0 dependence of $\langle S^2 \rangle_z^{1/2}$ for **cADMPCi31K** (filled square) and **ADMPCi130K** (filled circle) in MEA at 25 °C along with the literature data for cADMPC [12] (unfilled squares) and ADMPC [17] (unfilled circles).

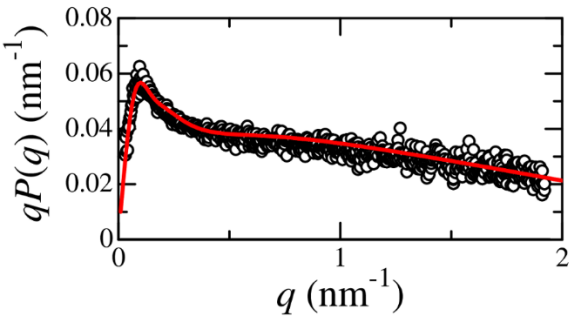

Fig. 5. Holtzer plots for **ADMPCi130K** in MEA at 25 °C. A solid curve indicates theoretical values for the wormlike cylinder model [23].

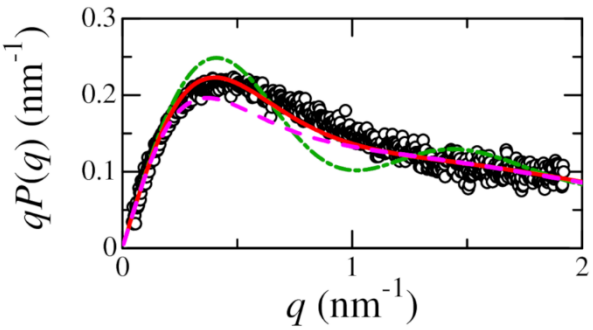

Fig. 6. Holtzer plots for **cADMPCi31K** in MEA at 25 °C. A solid red curve indicates theoretical $P(q)$ values for the touched-bead wormlike ring model with $Đ = 1.20$. A dot-dashed green curve, theoretical values for the monodisperse wormlike ring. A dashed magenta curve, theoretical values for touched-bead rigid ring with $Đ = 1.20$.

3.2. Chiral separation behavior in n-hexane/2-propanol (9/1).

Some examples of the HPLC chromatograms are shown in Fig. 7 in which *n*-hexane/2-propanol (9/1) was used as the mobile phase. The column made of **cADMPC49K** clearly separates **d** while the **ADMPC49K** column shows a single peak with no chiral separation. On the contrary, only **ADMPC49K** column separates **f**. These results indicate that cADMPC and ADMPC have appreciably different chiral separation ability.

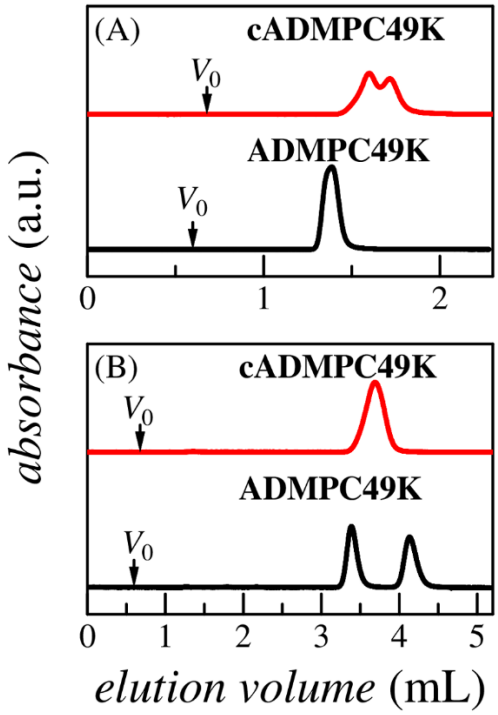

Fig. 7. Chromatograms of **d** (A) and **f** (B) on indicated CSPs using *n*-hexane/2-propanol (9/1) as the eluent. Arrows indicate the dead volume (V_0) of the column.

The modified separation factor α' defined as

$$\alpha' \equiv \frac{k_{E+}}{k_{E-}} \qquad (1)$$

were plotted against M_w in Fig. 8 instead of the conventional separation factor α to clarify the difference in the elution order among the investigated CSPs. Note that α is plotted for **h** because appropriate CD signal was not obtained. The error bar is based on the plate theory with the current N value [26, 27]. While the ADMPC columns (circles) appreciably separated **a**-**d**, **f**, and **g** as shown in Fig. 8, significant resolution for the cADMPC columns (squares) was found only for **a**, **b**, and **d** of which the elution order is the same as that for the linear chain. Interestingly, the resolution of **d** is better for the cADMPC columns than that for the ADMPC whereas the ADMPC column has higher resolution for the other racemates. This difference in the chiral separation clearly indicates that the topology of the polymer chains affects the chiral recognition of CSPs. Taking into consideration that the local helical structure of cADMPC is more extended than that for the linear chain [12], the local helical structure in the CSPs may play an important role for the chiral separation.

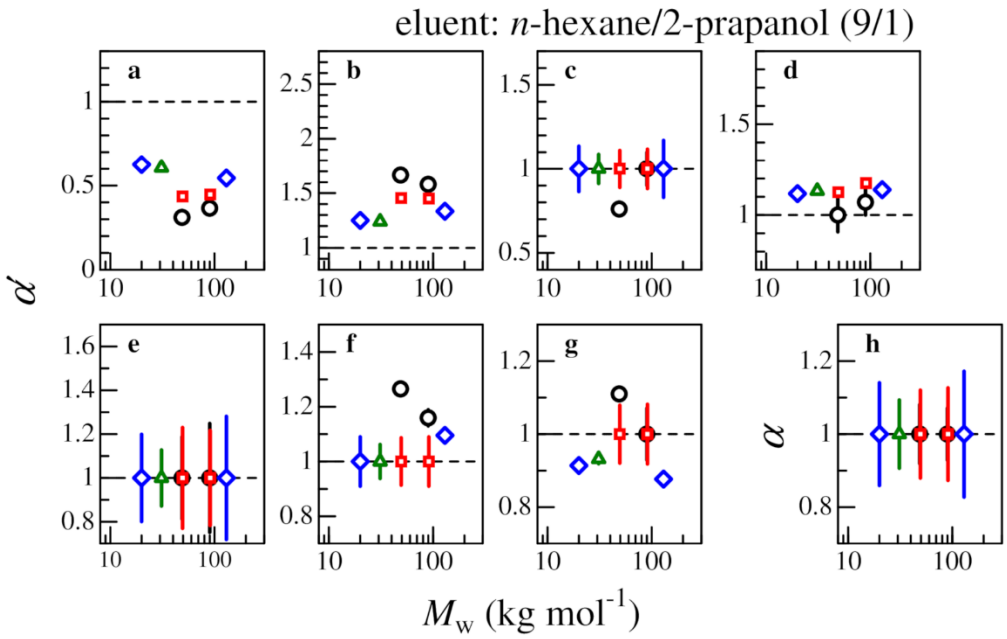

Fig. 8. M_w dependence of α' or α for the indicated racemates (**a**-**h**) separated on ADMPC columns (circles), cADMPC columns (squares), cADMPCi column (triangles), and ADMPCi columns (diamonds), with *n*-hexane/2-propanol (9/1) as the eluent.

Another important point is the chain length dependence of the resolution. Chiral separation ability for the ADMPC column systematically decreases and becomes close to that for the cADMPC chain with increasing M_w for **a**-**c**, **f**, and **g**. This is an opposite tendency to the above mentioned very low M_w ADMPC [13]. When a polymer chain is adsorbed on the silica gel in the physically coating process to form loops, trains, and tails [28-31], the conformational fluctuation may be restricted for the loop and train chains. The conformation of the loop chain of ADMPC

may be rather similar to that for the cADMPC chain, and the fraction of the loop chains should increase with increasing the molecular weight of ADMPC. It is however noticed that no significant chain length effects on chiral separation ability was detected for a cellulosic CSP made of cellulose tris(3,5-dimethylphenylcarbamate) except for very short chains [32, 33], suggesting this is a specific behavior for amylose based CSPs.

Next, we compare the chiral separation behavior for the coated-type columns with those for immobilized columns. The α' values of **a**-**c** and **f** for immobilized CSPs are appreciably closer to unity than those for the coated type CSPs while an opposite behavior is found for **d**. This tendency is quite similar to those for the cADMPC columns but the difference is more significant. Another interesting point is that the chiral separation behavior between ADMPCi and cADMPCi are quite similar. Furthermore, opposite elution order was found for **g**. The α values for ADMPCi are similar to the previous report [18]. Taking into consideration that the current ADMPCi and cADMPCi have relatively large amount of linker unit, the part chain between two adjacent linkers may bend more significantly and/or the local helical structure may be stretched more than the physically coated cADMPC chains. The difference in the linear and cyclic topology of the immobilized chain is consequently no more important for the local helical structure. It should be noted that the current result is different from the commercially available immobilized ADMPC columns of which linker contents is much lower than that for this study. Indeed, less significant difference between immobilized and coated columns were found when the linker content is lower [14, 34, 35].

3.3. Chiral Separation Behavior in n-Hexane/2-Propanol (99/1).

The α' value for **a**-**e** and **h** for the CPSs made of ADMPC, cADMPC, and ADMPCi in *n*-hexane/2-propanol (99/1) are plotted against M_w in Fig. 9. Relatively high chiral separation performance was observed for all the tested racemates including **e** and **h**, for which no appreciable resolution of the enantiomers was found in the former mobile phase. The elution order from the racemates does not depend on the investigated CSPs. Fig. 9 shows that the α' values of cADMPC are somewhat closer to $\alpha' = 1$ than those of ADMPC for **a** and **b**. For **c** and **h**, however, α' (α) for cADMPC is slightly larger. Interestingly, the difference in α' between cADMPC and ADMPC for **a**-**c** becomes the most significant for the middle M_w sample. This seemingly complex M_w dependence suggests that not only the local conformational difference plays an important role for the chiral separation but also chain end effects become more important with lowering M_w. The α' values of **d** and **e** for cADMPC and ADMPC are substantially close to each other whereas somewhat difference is found for the lowest M_w sample. This is reasonable because conformational difference between linear and ring chains becomes more significant with lowering M_w. It is noted that the elution order of the enantiomers for **c** in *n*-hexane/2-propanol (99/1) is opposite to that in *n*-hexane/2-propanol (9/1) and similar behavior with changing alcohol content was also reported in some previous studies [36-38].

Let us compare the α' (α) data with those for the immobilized CSPs. The α' values of ADMPCi are closer to unity than those of ADMPC for **a**-**d** while the α' values of ADMPCi are quite similar to those of cADMPC except for **c**. This similarity between the immobilized CSP and cyclic chain is comparable to the former result in *n*-hexane/2-propanol (9/1).

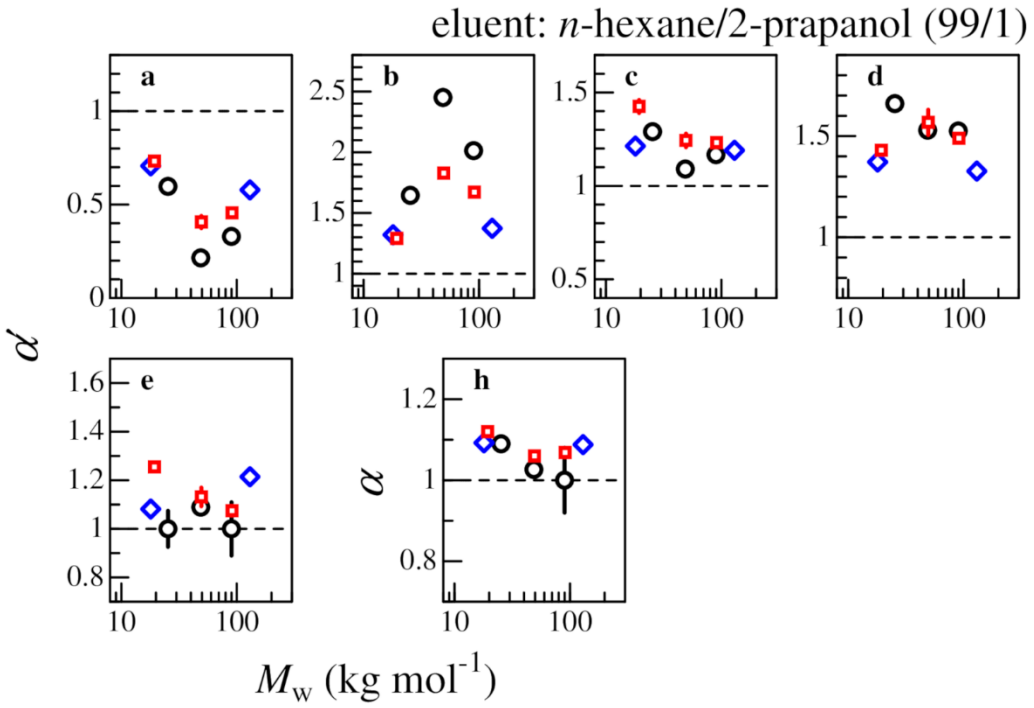

Fig. 9. M_w dependence of α' or α for the indicated racemates (**a**-**e** and **h**) separated on ADMPC CSPs (circles), cADMPC CSPs (squares), and ADMPCi CSPs (diamonds), with *n*-hexane/2-propanol (99/1) as the eluent.

3.4. Adsorption of analytes to the stationary phases.

The geometric average [$\bar{k} = (k_{E-}\, k_{E+})^{1/2}$] of the capacity factors may be associated with the mean of molar Gibbs energy of adsorption for the E– (ΔG_{E-}) and E+ (ΔG_{E+}) by the following equation [39],

$$\ln \bar{k} = \frac{\ln k_{E-} + \ln k_{E+}}{2} = -\frac{1}{RT}\left(\frac{\Delta G_{E-} + \Delta G_{E+}}{2}\right) + \ln \phi \qquad (2)$$

where ϕ denotes the volume ratio of the stationary to the mobile phase. The obtained $\bar{k}$ shown in Figs. S3 and S4 is substantially independent of the stationary phase while it significantly depends on the analyte, suggesting that local helical conformation of polysaccharide derivative molecules does not cause appreciable difference in the adsorption behavior of the racemates. In other words, chiral separation of the current stationary phases utilizes slight difference in the adsorption ability to polysaccharide derivative molecules between the enantiomers. The direct estimate of this adsorption ability (the preferential adsorption) for each pair of the polysaccharide derivative and the enantiomer is desirable to clarify the detailed mechanism. As an example, the preferential adsorption difference between D- and L-ethyl lactates to amylose tris(*n*-butylcarbamate) was detected by the isothermal calorimetry measurement [40].

4. Conclusion

Both coated and immobilized type chiral stationary phases (CSPs) consisting of cyclic amylose tris(3,5-dimethylphenylcarbamate) (cADMPC) were successfully prepared while their linear analogues were also prepared for comparison. The chiral separation ability of the coated-

type cADMPC CSPs is appreciably different from that for ADMPC, indicating local helical structure difference between the cyclic and linear amylose derivatives is substantially important for the performance as CSPs. On the other hand, the CSPs made of cADMPC have quite similar chiral separation behavior as those for the immobilized-type cADMPCi and ADMPCi columns when the linker content is quite high, suggesting that the local helical structure of the immobilized polysaccharide chains is rather similar to that for cADMPC. These results indicate that the local conformation of the polysaccharide derivatives plays an important role for the chiral separation behavior.

Acknowledgments
We are grateful to Professor Takahiro Sato at Osaka University for fruitful discussion, to Dr. Yuuya Nagata for column preparation, to Professor Yoshio Okamoto at Nagoya University for providing information for preliminary experiments for CSPs, to Dr. Shiho Suzuki, Dr. Makoto Nakaya, and Mr. Yoshihiro Umetani at Osaka Prefecture University, and Mr. Daigo Kabata at Osaka University for preparation of cyclic amylose samples, to Dr. Noboru Ohta at SPring-8 for SAXS measurements. The synchrotron radiation experiments were performed at the BL40B2 in SPring-8 with the approval of the Japan Synchrotron Radiation Research Institute (JASRI) (Proposal No. 2017B1062). This work was partly supported by JSPS KAKENHI Grant Numbers JP18J10648 and JP17K05884.

Appendix A. Supplementary data

^{1}H NMR spectrum for **cADMPCi31K**, ultimate analysis results for **ADMPC90K**, **cADMPCi31K**, **ADMPCi18K**, **ADMPCi20K**, and **ADMPCi130K**, CD spectra of each fraction of the separated racemates, tables for the all α' and $\bar{k}$ data, and plots for $\bar{k}$ against M_w for all tested racemates and columns.

References

[1] J. Shen, Y. Okamoto, Efficient Separation of Enantiomers Using Stereoregular Chiral Polymers, Chem. Rev., 116 (2016) 1094-1138, https://doi.org/10.1021/acs.chemrev.5b00317.
[2] T.D. Booth, I.W. Wainer, Investigation of the enantioselective separations of α-alkylarylcarboxylic acids on an amylose tris(3,5-dimethylphenylcarbamate) chiral stationary phase using quantitative structure-enantioselective retention relationships Identification of a conformationally driven chiral recognition mechanism, J. Chromatogr. A, 737 (1996) 157-169, https://doi.org/10.1016/0021-9673(96)00011-8.
[3] T.D. Booth, I.W. Wainer, Mechanistic investigation into the enantioselective separation of mexiletine and related compounds, chromatographed on an amylose tris(3,5-dimethylphenylcarbamate) chiral stationary phase, J. Chromatogr. A, 741 (1996) 205-211, https://doi.org/10.1016/0021-9673(96)00208-7.
[4] R. Kaliszan, Retention data from affinity high-performance liquid chromatography in view of chemometrics, J Chromatogr B Biomed Sci Appl, 715 (1998) 229-244, https://doi.org/10.1016/S0378-4347(98)00175-3.
[5] M. Markuszewski, R. Kaliszan, Quantitative structure-retention relationships in affinity high-performance liquid chromatography, Journal of chromatography. B, Analytical technologies in the biomedical and life sciences, 768 (2002) 55-66, https://doi.org/10.1016/S0378-4347(01)00485-6.

[6] C. Yamamoto, E. Yashima, Y. Okamoto, Structural analysis of amylose tris(3,5-dimethylphenylcarbamate) by NMR relevant to its chiral recognition mechanism in HPLC, J. Am. Chem. Soc., 124 (2002) 12583-12589, https://doi.org/10.1021/ja020828g.
[7] R.B. Kasat, Y. Zvinevich, H.W. Hillhouse, K.T. Thomson, N.H.L. Wang, E.I. Franses, Direct probing of sorbent-solvent interactions for amylose tris(3,5-dimethylphenylcarbamate) using infrared spectroscopy, X-ray diffraction, solid-state NMR, and DFT modeling, J. Phys. Chem. B, 110 (2006) 14114-14122, https://doi.org/10.1021/jp061892d.
[8] R.B. Kasat, E.I. Franses, N.-H.L. Wang, Experimental and Computational Studies of Enantioseparation of Structurally Similar Chiral Compounds on Amylose Tris(3,5-DimethylPhenylCarbamate), Chirality, 22 (2010) 565-579, https://doi.org/10.1002/chir.20791.
[9] C. West, Y. Zhang, L. Morin-Allory, Insights into chiral recognition mechanisms in supercritical fluid chromatography. I. Non-enantiospecific interactions contributing to the retention on tris-(3,5-dimethylphenylcarbamate) amylose and cellulose stationary phases, J. Chromatogr. A, 1218 (2011) 2019-2032, https://doi.org/10.1016/j.chroma.2010.11.084.
[10] C. West, G. Guenegou, Y. Zhang, L. Morin-Allory, Insights into chiral recognition mechanisms in supercritical fluid chromatography. II. Factors contributing to enantiomer separation on tris-(3,5-dimethylphenylcarbamate) of amylose and cellulose stationary phases, J. Chromatogr. A, 1218 (2011) 2033-2057, https://doi.org/10.1016/j.chroma.2010.11.085.
[11] S. Khater, Y. Zhang, C. West, Insights into chiral recognition mechanism in supercritical fluid chromatography III. Non-halogenated polysaccharide stationary phases, J. Chromatogr. A, 1363 (2014) 278-293, https://doi.org/10.1016/j.chroma.2014.06.084.
[12] A. Ryoki, H. Yokobatake, H. Hasegawa, A. Takenaka, D. Ida, S. Kitamura, K. Terao, Topology-Dependent Chain Stiffness and Local Helical Structure of Cyclic Amylose Tris(3,5-dimethylphenylcarbamate) in Solution, Macromolecules, 50 (2017) 4000-4006, https://doi.org/10.1021/acs.macromol.7b00706.
[13] R. Aburatani, Y. Okamoto, K. Hatada, Optical Resolving Ability of 3,5-Dimethylphenylcarbamates of Oligosaccharides and Cyclodextrins, Bull. Chem. Soc. Jpn., 63 (1990) 3606-3610, https://doi.org/10.1246/bcsj.63.3606.
[14] T. Ikai, C. Yamamoto, M. Kamigaito, Y. Okamoto, Immobilized Polysaccharide-Based Chiral Stationary Phases for HPLC, Polym. J., 38 (2006) 91, https://doi.org/10.1295/polymj.38.91.
[15] S. Kitamura, H. Yunokawa, S. Mitsuie, T. Kuge, Study on Polysaccharide by the Fluorescence Method .2. Micro-Brownian Motion and Conformational Change of Amylose in Aqueous-Solution, Polym. J., 14 (1982) 93-99, https://doi.org/10.1295/Polymj.14.93.
[16] Y. Nakata, K. Amitani, T. Norisuye, S. Kitamura, Translational Diffusion Coefficient of Cycloamylose in Aqueous Sodium Hydroxide, Biopolymers, 69 (2003) 508-516, https://doi.org/10.1002/bip.10393.
[17] M. Tsuda, K. Terao, Y. Nakamura, Y. Kita, S. Kitamura, T. Sato, Solution Properties of Amylose Tris(3,5-dimethylphenylcarbamate) and Amylose Tris(phenylcarbamate): Side Group and Solvent Dependent Chain Stiffness in Methyl Acetate, 2-Butanone, and 4-Methyl-2-pentanone, Macromolecules, 43 (2010) 5779-5784, https://doi.org/10.1021/ma1006528.
[18] T. Ikai, C. Yamamoto, M. Kamigaito, Y. Okamoto, Immobilization of polysaccharide derivatives onto silica gel Facile synthesis of chiral packing materials by means of intermolecular polycondensation of triethoxysilyl groups, J. Chromatogr. A, 1157 (2007) 151-158, https://doi.org/10.1016/j.chroma.2007.04.054.

[19] N. Shimizu, K. Yatabe, Y. Nagatani, S. Saijyo, T. Kosuge, N. Igarashi, Software Development for Analysis of Small-angle X-ray Scattering Data, AIP Conf. Proc., 1741 (2016) 050017, https://doi.org/10.1063/1.4952937.
[20] Y. Okamoto, R. Aburatani, T. Fukumoto, K. Hatada, Chromatographic Resolution .17. Useful Chiral Stationary Phases for Hplc - Amylose Tris(3,5-Dimethylphenylcarbamate) and Tris(3,5-Dichlorophenylcarbamate) Supported on Silica-Gel, Chem. Lett., 16 (1987) 1857-1860, https://doi.org/10.1246/Cl.1987.1857.
[21] J. Shen, T. Ikai, Y. Okamoto, Synthesis and chiral recognition of novel amylose derivatives containing regioselectively benzoate and phenylcarbamate groups, J. Chromatogr. A, 1217 (2010) 1041-1047, https://doi.org/10.1016/j.chroma.2009.07.027.
[22] I. Shimizu, A. Yoshino, H. Okabayashi, E. Nishio, C.J. O'Connor, Kinetics of interaction of 3-aminopropyltriethoxysilane on a silica gel surface using elemental analysis and diffuse reflectance infrared Fourier transform spectra, J. Chem. Soc., Faraday Trans., 93 (1997) 1971-1979, https://doi.org/10.1039/a608121e.
[23] Y. Nakamura, T. Norisuye, Scattering Function for Wormlike Chains with Finite Thickness, J. Polym. Sci., Part. B: Polym. Phys., 42 (2004) 1398-1407, https://doi.org/10.1002/polb.20026.
[24] R. Tsubouchi, D. Ida, T. Yoshizaki, H. Yamakawa, Scattering Function of Wormlike Rings, Macromolecules, 47 (2014) 1449-1454, https://doi.org/10.1021/ma402572k.
[25] A. Ryoki, D. Ida, K. Terao, Scattering function of semi-rigid cyclic polymers analyzed in terms of worm-like rings: cyclic amylose tris(phenylcarbamate) and cyclic amylose tris(n-butylcarbamate), Polym. J., 49 (2017) 633-637, https://doi.org/10.1038/pj.2017.27.
[26] V.R. Meyer, Practical High-Performance Liquid Chromatography: Fifth Edition, 2010.
[27] G.D. Christian, P.K. Dasgupta, K.A. Schug, Analytical chemistry, 7th ed., John Wiley & Sons, Hoboken, N.J., 2014.
[28] A.R. Khokhlov, F.F. Ternovsky, E.A. Zheligovskaya, Statistics of Stiff Polymer-Chains near an Adsorbing Surface, Makromol Chem-Theor, 2 (1993) 151-168, https://doi.org/10.1002/mats.1993.040020201.
[29] E.Y. Kramarenko, R.G. Winkler, P.G. Khalatur, A.R. Khokhlov, P. Reineker, Molecular dynamics simulation study of adsorption of polymer chains with variable degree of rigidity. I. Static properties, J. Chem. Phys., 104 (1996) 4806-4813, https://doi.org/10.1063/1.471175.
[30] T.A. Kampmann, J. Kierfeld, Adsorption of finite semiflexible polymers and their loop and tail distributions, J. Chem. Phys., 147 (2017) 014901, https://doi.org/10.1063/1.4990418.
[31] A.R. Hall, M. Geoghegan, Polymers and biopolymers at interfaces, Reports on progress in physics. Physical Society, 81 (2018) 036601, https://doi.org/10.1088/1361-6633/aa9e9c.
[32] N. Kasuya, Y. Kusaka, N. Habu, A. Ohnishi, Development of chiral stationary phases consisting of low-molecular-weight cellulose derivatives covalently bonded to silica gel, Cellulose, 9 (2002) 263-269, https://doi.org/10.1023/A:1021188610098.
[33] Y. Okada, C. Yamamoto, M. Kamigaito, Y. Gao, J. Shen, Y. Okamoto, Enantioseparation Using Cellulose Tris(3,5-dimethylphenylcarbamate) as Chiral Stationary Phase for HPLC: Influence of Molecular Weight of Cellulose, Molecules, 21 (2016) 1484, https://doi.org/10.3390/molecules21111484.
[34] T. Ikai, C. Yamamoto, M. Kamigaito, Y. Okamoto, Immobilized-type chiral packing materials for HPLC based on polysaccharide derivatives, J. Chromatogr. B. Analyt. Technol. Biomed. Life Sci., 875 (2008) 2-11, https://doi.org/10.1016/j.jchromb.2008.04.047.

[35] J. Shen, T. Ikai, Y. Okamoto, Synthesis and application of immobilized polysaccharide-based chiral stationary phases for enantioseparation by high-performance liquid chromatography, J. Chromatogr. A, 1363 (2014) 51-61, https://doi.org/10.1016/j.chroma.2014.06.042.
[36] C. Xiang, G. Liu, S. Kang, X. Guo, B. Yao, W. Weng, Q. Zeng, Unusual chromatographic enantioseparation behavior of naproxen on an immobilized polysaccharide-based chiral stationary phase, J. Chromatogr. A, 1218 (2011) 8718-8721, https://doi.org/10.1016/j.chroma.2011.10.014.
[37] S. Ma, S. Shen, H. Lee, M. Eriksson, X. Zeng, J. Xu, K. Fandrick, N. Yee, C. Senanayake, N. Grinberg, Mechanistic studies on the chiral recognition of polysaccharide-based chiral stationary phases using liquid chromatography and vibrational circular dichroism: reversal of elution order of N-substituted alpha-methyl phenylalanine esters, J. Chromatogr. A, 1216 (2009) 3784-3793, https://doi.org/10.1016/j.chroma.2009.02.046.
[38] I. Matarashvili, L. Chankvetadze, S. Fanali, T. Farkas, B. Chankvetadze, HPLC separation of enantiomers of chiral arylpropionic acid derivatives using polysaccharide-based chiral columns and normal-phase eluents with emphasis on elution order, J. Sep. Sci., 36 (2013) 140-147, https://doi.org/10.1002/jssc.201200885.
[39] M. Lammerhofer, Chiral recognition by enantioselective liquid chromatography: mechanisms and modern chiral stationary phases, J. Chromatogr. A, 1217 (2010) 814-856, https://doi.org/10.1016/j.chroma.2009.10.022.
[40] S. Arakawa, K. Terao, S. Kitamura, T. Sato, Conformational change of an amylose derivative in chiral solvents: amylose tris(n-butylcarbamate) in ethyl lactates, Polym. Chem., 3 (2012) 472-478, https://doi.org/10.1039/c1py00432h.